INVESTIGATION OF RADIATION DAMAGE TO THE Al_2O_3 / Si WAFER INTERFACE DURING ELECTRON BEAM EVAPORATION BY MEANS OF *C-V* AND LIFETIME MEASUREMENTS

Y. Schiele, G. Hahn, B. Terheiden
University of Konstanz, Department of Physics, P.O. Box X916, D-78457 Konstanz, Germany
Phone: +49 (0) 7531 88 4995, Fax: +49 (0) 7531 88 3895, Email: Yvonne.Schiele@uni-konstanz.de

ABSTRACT: For the purpose of reducing recombination activity in crystalline silicon solar cells, atomic layer deposited aluminum oxide (Al_2O_3) has proven a promising candidate. Its excellent surface passivation is effected by an exceptionally high density of negative fixed charges Q_f generating a strong field-effect along with a chemical passivation reducing the density of interface traps D_{it}. The dependence of these two measures on the temperature and the duration of the post-deposition anneal activating the passivation of Al_2O_3 is investigated by measuring the capacitance-voltage (*C-V*) characteristics. To directly correlate Q_f and D_{it} with the effective minority carrier lifetime τ_{eff}, a new kind of sample structure is developed, whereby both measurement types can be conducted on the same test sample. The interface properties of samples with thermal and electron beam evaporated metal contacts are compared and a correlation with the obtained passivation quality quantified by τ_{eff} is identified in order to investigate the influence of the radiation damage. It is found that Q_f, D_{it} and τ_{eff} of Al_2O_3 passivated *p*-doped Si wafers exhibit a correlation when annealing parameters are varied and that an electron beam evaporation of Al damages the Al_2O_3/Si interface and significantly reduces τ_{eff}. Finally, a method to restore the effective lifetime is developed and investigated which yields a recovery rate of 65% corresponding to a reduction of D_{it} and an increase of Q_f.
Keywords: Al_2O_3, Lifetime, *C-V*, Radiation Damage

1 INTRODUCTION

In recent years, atomic layer deposited Al_2O_3 has been proven to feature excellent surface passivation properties on *p*-type silicon wafers being the most common solar cell base material [1, 2]. Accordingly, Al_2O_3 is used as rear side dielectric passivation layer in high efficiency *p*-type silicon solar cells with local rear contacts established, for example, by laser-firing, thus known as Laser-Fired Contacts (LFC) [3].

The passivating character of Al_2O_3 on silicon surfaces is based on two pivotal mechanisms. On the one hand, the Al_2O_3 layer provides chemical passivation as it is able to saturate the dangling bonds on the silicon surface which previously exhibits a high density of interface states D_{it} in the silicon band gap [4, 5]. On the other hand, a high density of negative fixed charges up to the range of $Q_f = 10^{13}$ cm^{-2} has been evidenced in dielectric Al_2O_3 [5]. This high density of fixed negative charges induces field-effect passivation.

Potential techniques for the rear side metalization of dielectrically passivated silicon solar cells are thermal evaporation and electron beam evaporation. During electron beam evaporation, radiation damage raises the surface recombination velocity of surfaces coated with a thermal SiO_2 layer [6]. Instead of the latter, we therefore examine Al_2O_3 passivated Si wafer surfaces in respect of the metalization techniques' impact upon D_{it} and Q_f, being characteristic measures of passivated Si wafer surfaces.

2 EXPERIMENTAL

2.1 Characterization techniques

Electrical properties of the Al_2O_3/Si (100) interface like the density of interface traps and the density of fixed charges are investigated by capacitance-voltage (*C-V*) measurements on metal-oxide-semiconductor (MOS) structures [7]. From the *C-V* characteristic, the density of fixed charges Q_f can be calculated by

$$Q_f = \frac{C_{OX}}{q} \cdot \left(V_{FB} + \phi_{MS} \right), \tag{1}$$

wherein C_{OX} is the oxide capacitance determined in accumulation, q the elementary electric charge, V_{FB} the voltage under flatband conditions and ϕ_{MS} the difference between the work functions of metal and semiconductor.

Measuring the high frequency capacitance C_{hf} as well as the quasi-static capacitance C_{qs} as a function of the applied voltage to the MOS structure, the density of interface traps D_{it} is determined employing the following equation

$$D_{it} = \frac{C_{it}}{q} = \frac{1}{q}\left[\left(\frac{1}{C_{qs}} - \frac{1}{C_{OX}}\right)^{-1} - \left(\frac{1}{C_{hf}} - \frac{1}{C_{OX}}\right)^{-1}\right]. \tag{2}$$

The resulting passivation quality is quantified by the effective minority carrier lifetime τ_{eff} in the surface-passivated wafer determined by means of photoconductance decay (PCD) measurement [8], where

$$\frac{1}{\tau_{eff}} = \frac{1}{\tau_{bulk}} + \frac{2S_{eff}}{W} \tag{3}$$

with τ_{bulk} being carrier lifetime in the silicon bulk, S_{eff} representing effective surface recombination velocity and W denoting wafer thickness. For the calculation of S_{eff}, Auger recombination is neglected and thus infinite bulk lifetime τ_{bulk} is assumed for the float-zone wafers used yielding an upper limit of S_{eff}.

In order to be able to reliably correlate D_{it}, Q_f and τ_{eff}, a new sample design, which we name combined lifetime/*C-V* sample, is developed. After the Si wafer is passivated by an Al_2O_3 layer on both faces, lifetime measurements can be conducted on the symmetrical test sample. Subsequently, this lifetime sample is remanufactured to a MOS structure by applying spot-shaped Al gate contacts. In order to obtain a complete *C-V* sample, an ohmic contact is established on the rear by full area metalization and subsequent laser-firing the Al through the Al_2O_3 layer. The described test sample is depicted in Fig. 1, including this second step metalization.

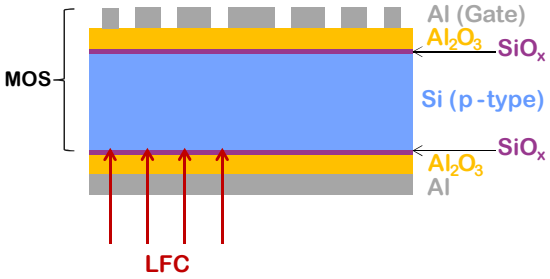

Figure 1: Schematic representation of a combined lifetime/*C-V* sample with both-sided Al_2O_3 passivation on top of silicon oxide interface layers. For *C-V* measurements, gate contacts on the front and, by laser-firing the Al through the Al_2O_3 layer, ohmic LFCs on the rear are established.

2.2 Fabrication of combined lifetime/*C-V* samples

In order to manufacture such test samples, first of all symmetrical lifetime samples are prepared from boron-doped, 5×5 cm^2 float-zone wafers with a specific resistivity of 2 Ωcm and a thickness of 250 or 525 µm. Manufacturing steps are illustrated in Fig. 2.

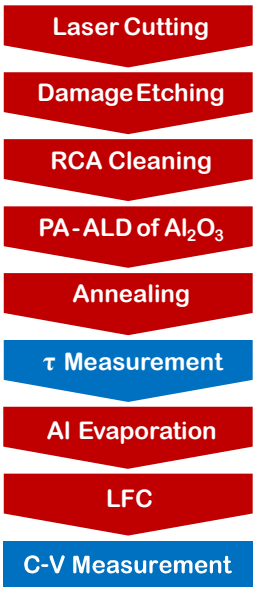

Figure 2: Manufacturing and characterization chronology of a combined lifetime/*C-V* sample.

These wafers, damaged by laser cutting, are etched in a chemical polishing solution [9], and afterwards the surface is subjected to a standard RCA cleaning step [10]. Then, Al_2O_3 layers with a thickness of 30 nm are deposited on both sides of the wafers by plasma assisted atomic layer deposition (PA-ALD) at ≈200 °C using a FlexAL device from Oxford Instruments. The thickness is verified by spectral ellipsometry. To "activate" the passivation property of the Al_2O_3 layers, an annealing step has been proven necessary [2].

In the first part of our analysis, the effect of this annealing step is investigated regarding various annealing temperatures between 340 and 470 °C as well as different annealing periods of 10 to 400 min in order to determine the settings for optimal passivation quality and to identify the respective electronic states at the Al_2O_3/Si interface. Processing Al_2O_3 passivated wafers, the thickness of the passivation layer represents another parameter. In this context, investigations concerning passivation quality, Q_f and D_{it} were carried out by Werner [11].

With our lifetime samples, photoconductance decay measurements are conducted and the effective minority carrier lifetime τ_{eff} is determined (eq. 3) at an injection density of $\Delta n = 10^{15}$ cm^{-3} utilizing a Sinton Lifetime Tester. In order to get a spatially resolved image of the carrier recombination activity, photoluminescence (PL) measurements are carried out. Thereby, it has to be taken into account that, due to metrological properties of the setup employed, a higher signal is measured at the center of samples with high lifetimes and that identical colors in different images cannot be assigned to the same lifetime value. However, for the investigations in this work, the knowledge of the qualitative PL signal distribution is sufficient.

After lifetime measurement, the passivated wafers are processed to *C-V* samples. For this purpose, using a shadow mask, Al gate contacts (area ≈ 1 mm^2) are evaporated on top of the Al_2O_3 layer on the front of each sample to create a MOS structure needed for *C-V* measurements. On the rear, Al is evaporated over the entire surface.

In the initial part of the experiment, all metal contacts of the samples are thermally evaporated. In the second part, the Al contacts are deposited using an electron beam evaporator in order to investigate the influence of different physical vapor deposition methods upon the Al_2O_3/Si interface properties. The ohmic contact on the rear side through the Al_2O_3 layer is established by means of the Laser-Fired Contacts (LFC) technique. Finally, the sample is used for capacitance-voltage profiling. The *C-V* measurements are performed in high-frequency [12] and quasi-static [13] mode which allows the calculation of Q_f in the Al_2O_3 layer at the interface to the silicon (eq. 1) and the calculation of D_{it} (eq. 2).

3 RESULTS

3.1 Process parameter variation

The first part of our analysis shows that the setting temperature of the 30 minute annealing step after Al_2O_3 deposition has significant influence on the passivation quality. This is evidenced by the measured effective lifetime of the different samples.

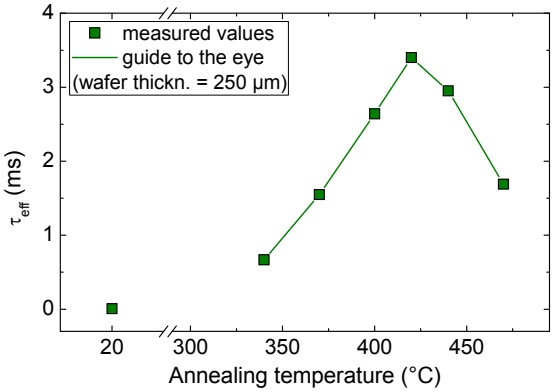

Figure 3: Effective minority carrier lifetime τ_{eff} after 30 minute annealing versus annealing temperature set.

Fig. 3 represents that without any annealing, this lifetime is below 10 µs. With increasing temperature, effective lifetime continuously increases and reaches its maximum at an annealing temperature set at 420 °C. Above this temperature, passivation quality decreases.

The PL images of the samples annealed at different temperatures are exhibited exemplarily in Fig. 4. The sample annealed at 420 °C features a very homogeneous distribution of PL signal neglecting measurement artifacts which corresponds very well to the maximum τ_{eff} value in Fig. 3. With decreasing temperatures an augmented number of small areas with a lower PL signal occurs. With increasing temperatures above 420 °C, the PL signal decreases extensively, originating from the edges.

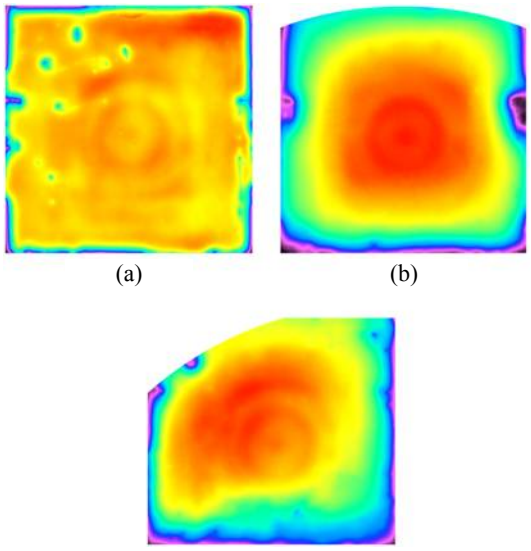

Figure 4: PL images of the samples annealed at (a) 340 °C, (b) 420 °C and (c) 470 °C. Purple is tantamount to high, red to low recombination activity. The scaling of the three wafers is not identical.

In order to examine whether metalization by thermal evaporation of Al changes passivation quality, the Al layers are etched away from metalized wafers (without LFC) by means of a hydrochloric acid (HCl) solution; subsequently, carrier lifetime is measured. It has been found that thermal evaporation is a damage-free deposition technique since the τ_{eff} values obtained by PCD measurement as well as the PL images of the recombination activity distribution before and after the metalization step do not diverge [14]. Hence, results derived from lifetime measurements before the metalization step can be correlated to results calculated from *C-V* measurements after the metalization step.

In Fig. 5 the density of negative fixed charges in the Al_2O_3 layer and the interface trap density in the middle of the Si energy gap both extracted from the *C-V* curves of a combined lifetime/*C-V* sample are represented versus the annealing temperature. The course of the curves reveals the reason for the temperature dependence of the Al_2O_3 passivation quality.

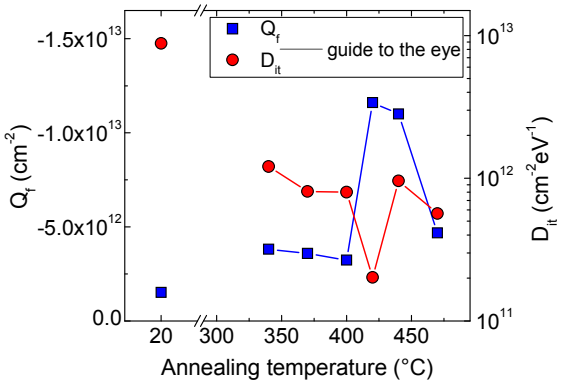

Figure 5: Density of fixed charges (left ordinate) and density of interface traps (right ordinate) at midgap after 30 minute annealing versus annealing temperature set.

Without any annealing step, only a very low density of fixed charges is detectable. Annealing at 340 °C raises the value of Q_f only marginally. The greatest increase is observable at an annealing temperature between 400 and 420 °C. The sample annealed at 420 °C features a density of fixed charges of $Q_f = 1.2\times10^{13}$ cm^{-2}.

The density of interface traps without an annealing step is very high at almost 1×10^{13} cm^{-2}eV^{-1}. Even an annealing step at only 340 °C reduces the D_{it} value by one order of magnitude. The minimum is observable at the same temperature at which Q_f reaches its maximum, namely at 420 °C, where effective lifetime is maximal, too.

From experiments dealing with the dependence of the minority carrier lifetime of samples coated with Al_2O_3 layers and accumulatively subjected to different annealing periods, it can be deduced that the passivation quality of Al_2O_3 depends on the duration of the annealing step as well.

Fig. 6 displays that only ten minutes at 420 °C are needed to increase τ_{eff} from below 10 µs to 3.4 ms which, with a wafer thickness of 250 µm, corresponds to an effective surface recombination velocity of 3.7 cm/s. After a total annealing period of 30 min, effective lifetime reaches its maximum, subsequently decreasing with additional annealing steps.

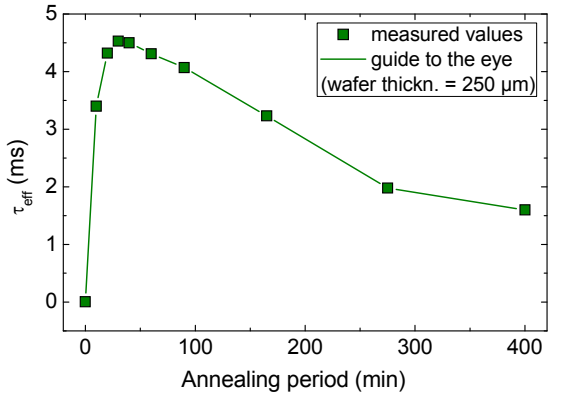

Figure 6: Effective minority carrier lifetime τ_{eff} after annealing at 420 °C versus accumulated annealing period.

In Fig. 7 the significant change in the density of fixed charges and the density of interface traps at midgap during the first ten minutes of annealing is illustrated. For longer annealing periods Q_f is nearly stable. D_{it} increases after approximately 150 min to 2×10^{12} $cm^{-2}eV^{-1}$.

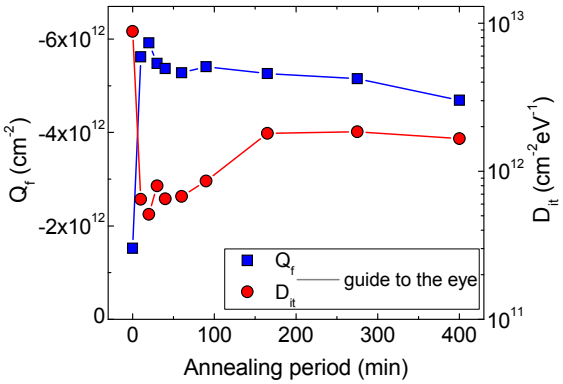

Figure 7: Density of fixed charges (left ordinate) and density of interface traps at midgap (right ordinate) after annealing at 420 °C versus accumulated annealing period.

3.2 Electron beam evaporated contacts

In its second part, our analysis examines whether the deposition of Al contacts by means of an electron beam evaporator influences the Al_2O_3/Si interface of the combined lifetime/*C-V* samples. For this purpose, sister samples are manufactured, one for measuring lifetime, and one for *C-V* measurement. From the lifetime sample, the Al is etched off the surface again after electron beam evaporation so that lifetime can be measured afterwards.

In fact, a damage of the samples can be identified from τ_{eff} measurements represented in Fig. 8. The effective lifetime of the Al_2O_3 coated sample after a post-deposition annealing step at 420 °C is more than 9 ms, which, with a wafer thickness of 525 µm, corresponds to an effective surface recombination velocity of 2.7 cm/s.

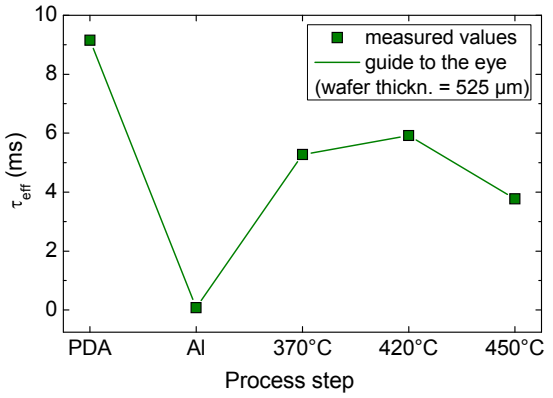

Figure 8: Effective minority carrier lifetime τ_{eff} versus subsequent process stages: post-deposition anneal (PDA; 420 °C, 30 min), Al electron beam evaporation and its subsequent etching off, 30 minute annealing at various temperatures.

After treatment in the electron beam evaporator, τ_{eff} falls to less than 100 µs. Thus, in contrast to thermal evaporation, depositing Al contacts by means of an electron beam evaporator damages the Al_2O_3/Si interface of the combined lifetime/*C-V* samples. The damage could have been caused by high-energetic particles or X-rays. These are thought to have damaged SiO_2 passivated silicon wafers during electron beam evaporation [6].

Furthermore, it is demonstrated that an annealing step at different temperatures between 370 and 450 °C can raise τ_{eff} again up to approximately 6 ms, which corresponds to a recovery rate of 65%.

The respective PL images at the different process stages (Fig. 9) depict the spatial distribution of lifetime.

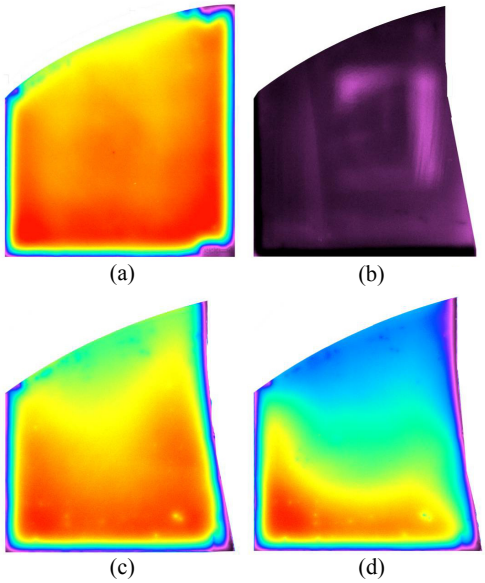

Figure 9: PL images after (a) post-deposition anneal, (b) electron beam evaporation and etching of Al, (c) 420 °C anneal and (d) 450 °C anneal. Purple is tantamount to high, red to low recombination activity. The scaling of the wafers is not identical.

Whereas directly after the post-deposition anneal (a) the sample shows a homogeneous high passivation quality, the measurement signal after evaporation and removal of Al (b) consists only of measurement artifacts. Annealing at 420 °C (c) partly recovers the passivation quality, whereupon at higher annealing temperatures (d) the recombination activity increases again in a large area.

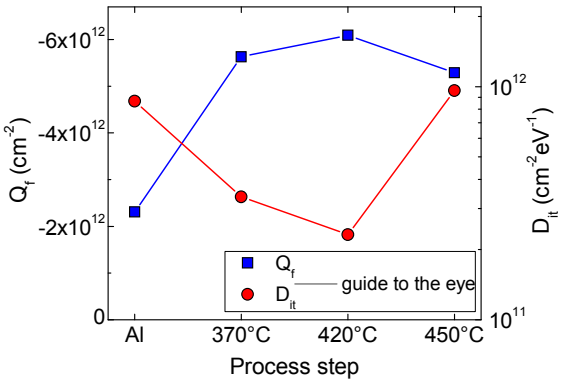

Figure 10: Density of fixed charges (left ordinate) and density of interface traps at midgap (right ordinate) versus subsequent process stages: Al electron beam evaporation, 30 minute annealing at various temperatures.

In order to check the electrical interface properties, Q_f and D_{it} are determined on the *C-V* sister sample after each of the process stages. The course of the Q_f curve features a shape similar to the one of the τ_{eff} values which once more evidences the correlation between these two quantities (Fig. 10). The D_{it} values determined in the middle of the Si energy gap develop inversely explaining the τ_{eff} values.

4 CONCLUSION

Atomic layer deposited Al_2O_3 is extraordinarily effective at minimizing recombination activity in crystalline silicon solar cells. Q_f and D_{it}, indicating passivation quality of Al_2O_3 layers on Si wafers, are determined by measuring the capacitance-voltage characteristics.

In order to directly correlate Q_f and D_{it} with the resulting effective carrier lifetime τ_{eff}, a new kind of sample structure, the "combined lifetime/*C-V* sample", has been developed. This structure allows measuring all three quantities on the same sample.

Q_f, D_{it} and τ_{eff} of Al_2O_3 passivated *p*-doped Si wafers have been evidenced to exhibit an explicit correlation when applying various annealing temperatures and periods. Furthermore, electron beam evaporation of Al has been found to damage the Al_2O_3/Si interface and to significantly reduce τ_{eff}. Eventually, a method to recover effective lifetime has been developed and investigated. This method yields a recovery rate of 65% corresponding to a reduction of D_{it} and an increase of Q_f.

5 ACKNOWLEDGEMENTS

The authors would like to thank N. Brinkmann and T. Lüder for fruitful discussions. The financial support for parts of this work by German BMU under contracts FKZ 0325168 and FKZ 0325079 is gratefully acknowledged. The content of this publication is the responsibility of the authors.

6 REFERENCES

[1] G. Dingemans et al., Proc. 5th WCPEC, Valencia, (2010), 1083
[2] B. Hoex et al., Appl. Phys. Lett. 89 (2006), 042112
[3] E. Schneiderlöchner et al., Prog. Photovolt.: Res. Appl. 10 (2002), 29
[4] B. Hoex et al., J. Appl. Phys. 104 (2008), 113703
[5] G. Agostinelli et al., Sol. En. Mat. & Solar Cells 90 (2006), 3438
[6] J. Kopp et al., Proc. 22nd IEEE PVSC (1991), 278
[7] S. M. Sze, *Physics of Semicond. Devices* (1981)
[8] R. A. Sinton et al., Appl. Phys. Lett. 69 (1996), 2510
[9] A. F. Bogenschütz, *Ätzpraxis für Halbleiter*, (1967)
[10] W. Kern, J. Electrochem. Soc. 137 (1990), 6
[11] F. Werner et al., J. Appl. Phys. 109 (2011), 113701
[12] D. K. Schroder, *Semiconductor Material and Device Characterization* (2006), p. 61ff
[13] R. Castagné, C. R. Hebd. Séanc. Acad. Sci. Paris 267 (1968), 866
[14] Y. Schiele, *Charakterisierung von Al_2O_3-Schichten zur Oberflächenpassivierung für kristalline Si-Solarzellen*, Diploma thesis, University of Konstanz (2011)